ResearchGate

See discussions, stats, and author profiles for this publication at:
http://www.researchgate.net/publication/234833286

Photoluminescence and Raman Scattering in Wet Chemically Etched Silicon Nanowires

ARTICLE *in* JOURNAL OF NANOELECTRONICS AND OPTOELECTRONICS · DECEMBER 2011

Impact Factor: 0.37 · DOI: 10.1166/jno.2011.1205

CITATIONS
8

6 AUTHORS, INCLUDING:

Kirill Alexandrovich Gonchar
Lomonosov Moscow State University
16 PUBLICATIONS **37** CITATIONS

SEE PROFILE

L. A. Golovan'
Lomonosov Moscow State University
102 PUBLICATIONS **550** CITATIONS

SEE PROFILE

Vladimir Sivakov
Leibniz-Institut für Photonische Tech…
52 PUBLICATIONS **740** CITATIONS

SEE PROFILE

Silke Christiansen
Helmholtz-Zentrum Berlin
287 PUBLICATIONS **3,356** CITATIONS

SEE PROFILE

Available from: Kirill Alexandrovich Gonchar
Retrieved on: 02 September 2015

Copyright © 2011 American Scientific Publishers
All rights reserved
Printed in the United States of America

Journal of
Nanoelectronics and Optoelectronics
Vol. 6, 519–524, 2011

Photoluminescence and Raman Scattering in Arrays of Silicon Nanowires

V. Yu. Timoshenko[1,*], K. A. Gonchar[1], L. A. Golovan[1], A. I. Efimova[1], V. A. Sivakov[2], A. Dellith[2], and S. H. Christiansen[3]

[1] Department of Physics, Moscow State M.V. Lomonosov University, 119991 Moscow, Russia
[2] Institute of Photonic Technology, D-07745 Jena, Germany
[3] Max Planck Institut für die Physik des Lichts, D-91054 Erlangen, Germany

Arrays of silicon (Si) nanowires with mean diameters of about 50–100 nm formed by wet-chemical etching of crystalline silicon wafers with low and high doping levels were investigated by means of photoluminescence and Raman spectroscopy. The photoluminescence bands in the spectral ranges of 650–900 nm and about 1100 nm were detected and explained by the radiative recombination of excitons confined in Si nanocrystals on the surface of Si nanowires and by the interband photoluminescence in the volume of Si nanowires, respectively. The intensities of the band-gap related photoluminescence and Raman scattering under excitation at 1064 nm were significantly larger for the Si nanowire samples in comparison with that for the crystalline Si substrates. This fact is explained by strong scattering of the excitation light, which results in partial light trapping in silicon nanowire arrays. The doping level and surface orientation of the substrate were found to influence the photoluminescence and Raman scattering in Si nanowire arrays.

Keywords: Silicon Nanowires, Raman Spectroscopy, Photoluminescence, Light Scattering.

1. INTRODUCTION

One-dimensional structures such as nanowires, nanobelts and nanotubes have gained tremendous attention within the last decades because of plenty of the interesting physical and chemical properties. Semiconductor nanowires caused particular interest due to their potential use in optoelectronics, photonics, photovoltaics, and sensor applications.[1–7] For all device concepts based on Si nanowires (SiNWs) it is of great importance to control the structure, electronic and optical properties of SiNWs. These properties are usually determined by formation method and post-treatment of SiNWs. The first method of SiNW formation based on vapour–liquid–solid growth (VLS) catalyzed by noble metal was proposed fifty years ago.[8] The VLS growth results in formation of well-oriented along the crystallographic directions SiNWs with diameters above 10 nm and the wire orientation is size-depended.[4] Disordered SiNWs with smaller diameters can be obtained by electrochemical etching of crystalline Si (*c*-Si) substrates in hydrofluoric acid (HF) solutions through growing highly porous Si layer (see for example, Refs. [9, 10]). Recently it was reported a new method of the growth of rather ordered SiNWs with diameters from 10 to 100 nm by using wet chemical etching (WCE) of *c*-Si wafers in HF-based solutions.[11] This method consists of several stages as (i) deposition of silver (Ag) layers or nanoparticles on *c*-Si substrate, (ii) red-ox reactions at Ag/Si interface, and (iii) chemical removal of residual Ag spices in nitric acid solution. The WCE growth possesses some advantages in comparison with other above mentioned methods because of possibilities to grow SiNWs on both bulk *c*-Si wafers and thin Si layers (e.g., multicrystalline, nanocrystalline or amorphous) on glass substrates.[12] It was found that SiNWs formed by the WCE method showed room temperature photoluminescence (PL) in the visible spectral range.[11,12] The most pronounce explanation for the room temperature PL was related to the quantum confinement effect that originates from nanoscaled roughness of SiNW sidewalls.[13] Both the PL and Raman scattering are widely used techniques for characterization of semiconductor structures. Ordering of SiNWs can result in preferential polarization of the PL emission and Raman scattering as it was demonstrated in the case of porous silicon.[14,15] While the polarization properties of PL of WCE-grown SiNWs are still not explored, the ordering of SiNWs and complicate structure of their surface regions should be considered. In the present paper,

*Author to whom correspondence should be addressed.

the PL and Raman scattering spectra of SiNWs are investigated with a special interest to the effects of nanowire arrays on the efficiency and polarization properties of PL and Raman signals. The study is focused on the near-infrared PL caused by the radiative processes in cores of SiNWs that allows us to compare them with corresponding properties of *c*-Si substrates.

2. EXPERIMENTAL DETAILS

Lightly and heavily doped *c*-Si wafers with the crystallographic orientation of surfaces along (100) and (111) directions were used as substrates for the SiNWs growth (see Table I and Refs. [11, 12] for more details). The substrates were cleaned by rinsing in acetone for 2 min followed by an ethanol rinse for 2 min. Native SiO_2 coverage was removal by a short dip in 40% HF solution followed by a 2% HF rinse for 1 min. Finally, the substrates were rinsed in de-ionized water and blow-dried with nitrogen. In the first step of the employed WCE method, Ag nanoparticles of different morphology were deposited on surfaces of the substrates by immersing them in aqueous solution of 0.02 M of silver nitrate ($AgNO_3$) and 5 M of HF in the volume ratio of 1:1 (solution I) for 30 sec. In the second step, the *c*-Si substrates covered with Ag nanoparticles were immersed in a 50 ml of the solution containing 5 M of HF and 30% H_2O_2 in the volume ratio 10:1 (solution II) in a teflon vessel for 1 h at room temperature. Finally, the substrates treated with solution I and II were rinsed several times in de-ionized water and dried at room temperature. The arrays were washed in a concentrated (65%) nitric acid (HNO_3) for 15 min to remove residual Ag nanoparticles from the SiNW surfaces.

Delivered by Ingen
Alexander Balan
IP: 169.235.12
Sun, 25 Dec 2011 2
AMERICAN SCIENTIFIC PUBLISHERS

The structure analysis of the prepared SiNWs was carried out by using a JEOL JSM-6300F field emission scanning electron microscope (SEM). The morphology of SiNWs was found to be depended on the orientation and doping type of *c*-Si substrates. Figure 1 shows SEM micrographs of the samples, which indicate the preferential orientation of SiNWs along the [100] direction. Indeed, SiNWs grown on the (100)-oriented substrate are characterized by better ordering along to the normal direction to the substrate surface (Fig. 1(b)). Also, for the samples prepared on the (111)-oriented substrates the transition from the [111] to [100] etching directions results in zig–zag architecture of SiNWs, as shown in Figures 1(a, c). The formation of more dense silicon nanowire structures was observed for sample #2 as shown in Figure 1(b). The mean sizes of diameters of SiNWs are 50–100 nm and the thickness of etched profile is about 40 μm.

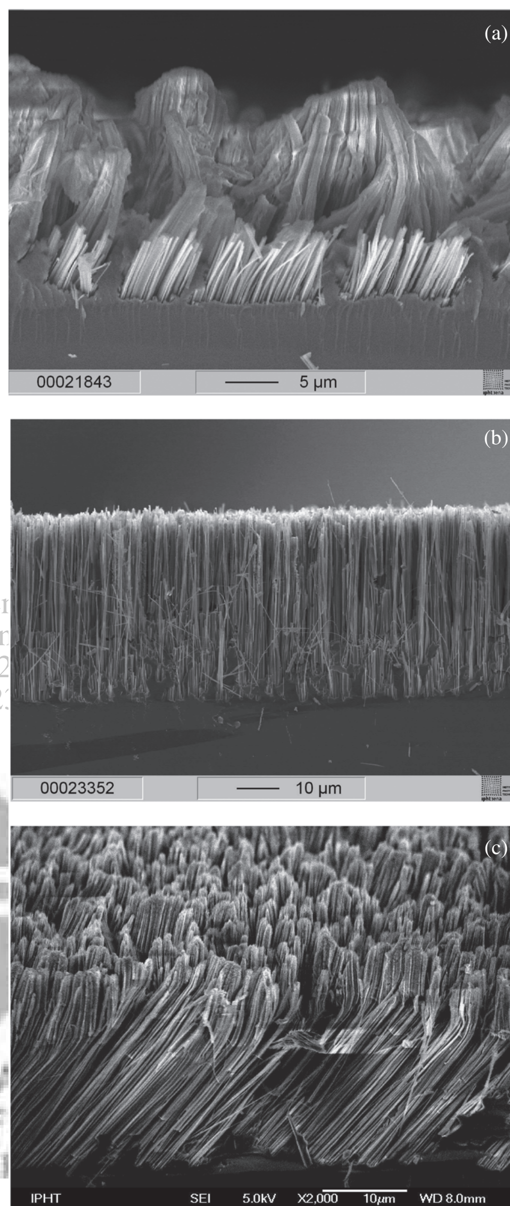

Fig. 1. Cross sectional SEM images of SiNWs samples #1 (a), #2 (b), and #3 (c).

Table I. Description of the investigated samples of SiNWs.

Sample	Length of SiNW (μm)	Substrate		
		Conductivity type: doping impurity	Surface orientation	Specific resistivity ($\Omega * $cm)
#1	25–30	*n*-Si:As	(111)	< 0.005
#2	40	*p*-Si:B	(100)	0.7–1.5
#3	30	*p*-Si:B	(111)	1–20

PL in the spectral region of 600 to 1300 nm was excited by the second harmonics of a Nd:YAG laser radiation (wavelength of 532 mm, power of 5 mW) and detected by a spectrometer equipped with a CCD array. A Fourier-transform infrared (FTIR) spectrometer (Bruker 66/vS) equipped with a Raman module (FRA106/S) was employed for the Raman-scattering and infrared photoluminescence (PL) measurements. A notch filter was employed to reject the excitation line in the registered

signal. Both the Raman scattering and PL were excited by cw radiation of a Nd:YAG laser at 1.064 μm with the power varied between 0 and 250 mW. The diameter of laser spot on the sample was about 2 mm. The dependences of the PL and Raman signals on the pumping laser radiation, which are important for understanding the nature of PL, were obtained for the samples of different doping levels. The measurements were done at normal laser radiation incidence and the detected PL and Raman signals were polarized perpendicular to the polarization of the excitation radiation (*s*-polarized laser radiation, *p*-polarized Raman and PL signals). To study the polarization properties of the PL and Raman signals in SiNWs the dependences of *s*- and *p*-polarized signals on polarization the excitation laser radiation for the incident angle of 75° was obtained, the results were compared with ones for the corresponding substrates (i.e., initial untreated *c*-Si wafers. A half-wave plate and Glan-Tailor prism analyzers were employed to control the polarization states of the excitation light and optical response of the samples, respectively. The experiments were carried out in air at room temperature.

Delivered by Ingenta to:
Alexander Balandin
IP : 169.235.12.9
Sun, 25 Dec 2011 23:48:47

3. RESULTS AND DISCUSSION

Both the visible and near-infrared PL spectra of the samples under excitation at 532 nm are shown in Figure 2. It is worth noting the broad PL band in the spectral region from 650 to 900 nm, which occurs in sample #1 and absent in the samples formed on the substrates with lower doping levels. This nearly visible PL, which was previously observed in SiNWs,[13] is likely caused by the radiative recombination of excitons confined in Si nanocrystals at the SiNW surfaces. The significantly larger PL intensity of sample #1 (see Fig. 2(a)) can be explained by more efficient processes of the local chemical etching on the SiNW surfaces (e.g., stain etching process[9]) because of the larger concentration of free charge carriers and defects in heavily doped SiNWs.

Besides the nearly visible PL band there is the near-infrared (NIR) PL with the spectral maximum at 1120–1150 nm, which was detected for the samples of SiNWs under excitation at 532 nm (Fig. 2). The PL intensity of the

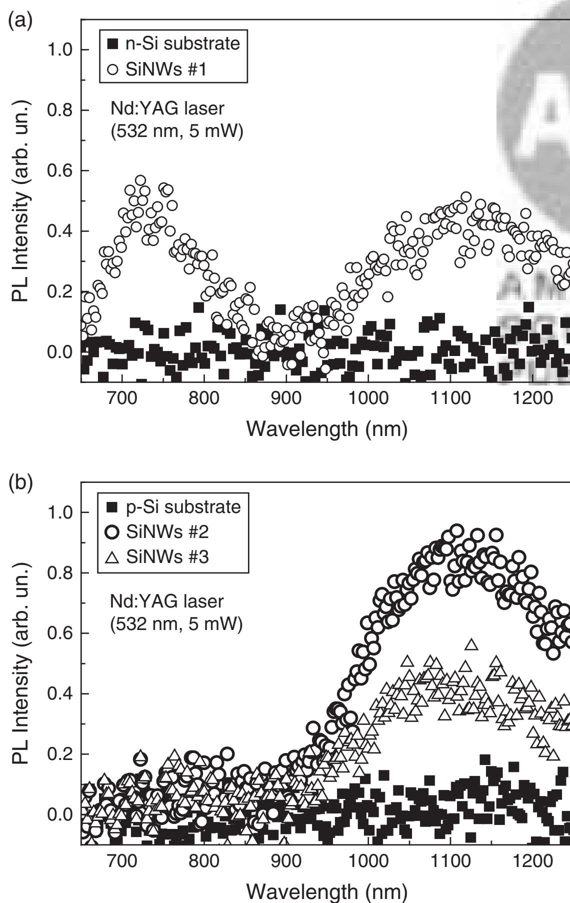

Fig. 2. Photoluminescence spectra of the substrates and SiNWs samples #1 (a) and #2, #3 (b) under excitation at 532 nm.

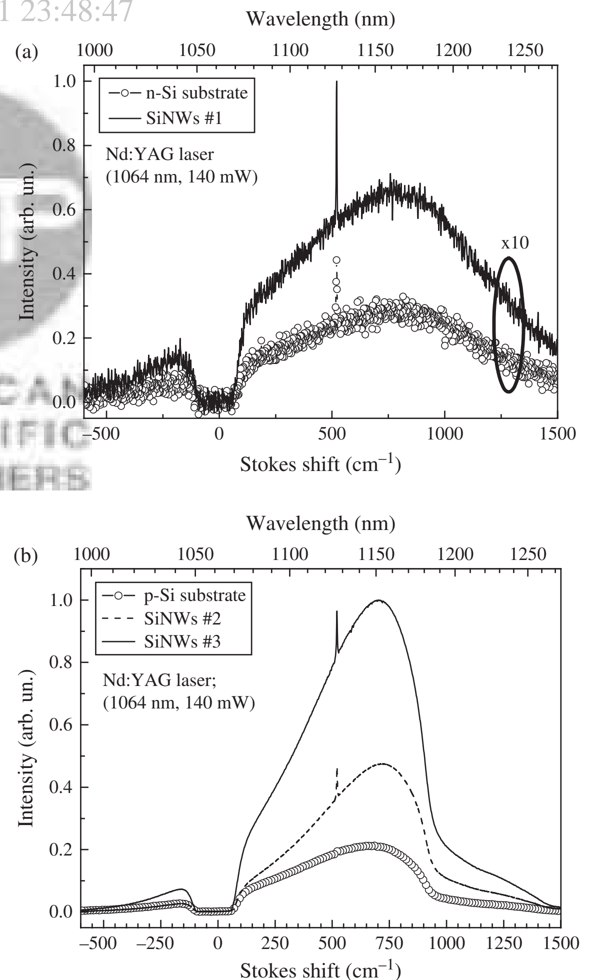

Fig. 3. Photoluminescence and Raman spectra of the substrates and SiNWs samples #1 (a) and #2, #3 (b) under excitation at 1064 nm. The excitation radiation was *s*-polarized.

NIR band was much higher than that for the corresponding *c*-Si substrates. The NIR PL band can be attributed to the inter-band radiative recombination of photoexcited charge carriers in the volume of SiNWs. The similar PL was observed in mesoporous Si formed by anodic etching of *c*-Si in HF-based solutions.[9, 16]

The NIR PL and Raman spectra of SiNW arrays and *c*-Si substrates excited at 1064 nm are presented in Figure 3. All PL spectra demonstrate a broad band from 1000 to 1250 nm. The intensity of the PL signal of the substrate of heavily doped *n*-Si(111)As wafer is much weaker comparing to lowly doped *p*-Si (100) or *p*-Si(111) wafers (cf. Figs. 3(a and b)). Additionally sharp peaks of the Raman scattering at 520 cm^{-1} are observed for the SiNWs samples and *c*-Si substrates. No anti-Stokes peaks were detected as shown in Figures 3(a, b) that evidences low heating effect at the employed laser radiation (intensity lower than 5 W/cm^2). Both the PL and Raman scattering intensities for sample #1 were found two-times higher than ones for the substrate of heavily doped *n*-Si:As (Fig. 3(a)). For samples #2 and #3 the PL signals increase by the factor of 2 and 5, correspondingly, whereas the intensity of Raman signal increases an order of magnitude in comparison with the corresponding substrates (Fig. 3(b)).

Dependences of the PL intensity on the excitation power for the samples and *c*-Si substrates are shown in Figure 4 in the double-logarithmic plots. For sample #1 and its substrate the dependence is linear, whereas samples #2, #3 and their substrates posses super-linear dependences of the PL signals on the laser power with slopes (i.e., exponent in the power low dependence) about 2. The difference in the excitation dependent PL intensities of the samples prepared on the heavily and lightly doped substrates can be explained by higher concentration of equilibrium charge carriers in the former samples, which strongly influence the recombination statistics of the photoexcited charge carriers. Indeed, the inter-band radiative recombination is obviously controlled by the interaction of the non-equilibrium charge carriers with equilibrium ones in heavily doped semiconductors. The same dependences for the SiNS sample and its substrate indicate the similar concentration of equilibrium charge carries. Besides, sample #3 exhibit well-expressed PL signal saturation at the laser power above 200 mW. This effect can be caused by an influence of the non-radiative Auger

Delivered by Ingenta to:
Alexander Balandin
IP : 169.235.12.9
Sun, 25 Dec 2011 23:48:47

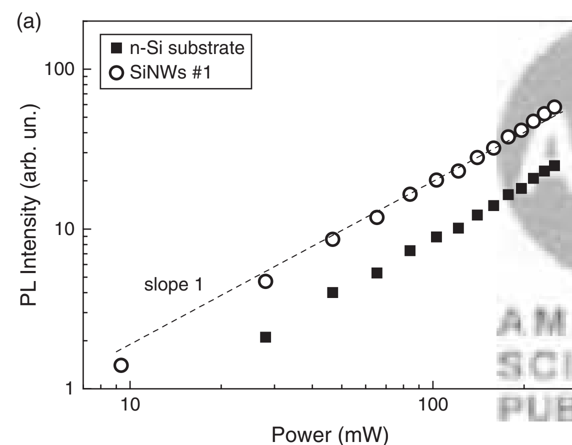

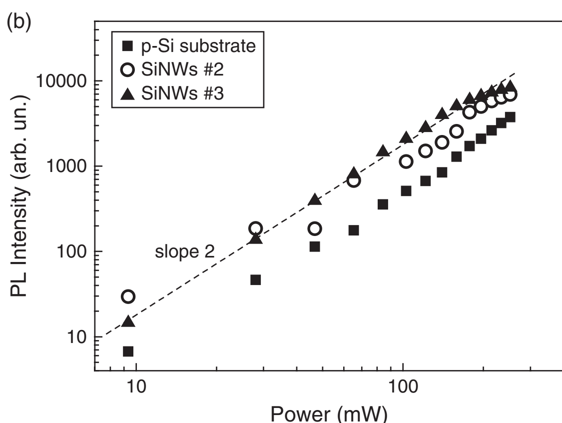

Fig. 4. Dependence of the photoluminescence intensity at 1125 nm on power of the excitation light at 1064 nm for SiNWs samples #1 (a), #2 and #3 (b), and for the corresponding substrates. Dashed lines in panels (a) and (b) represent linear and quadratic dependences, respectively.

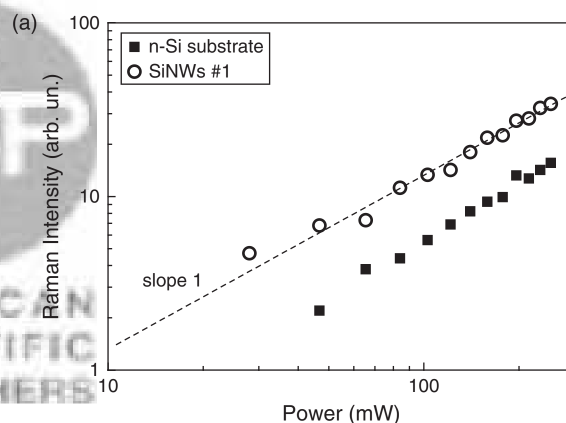

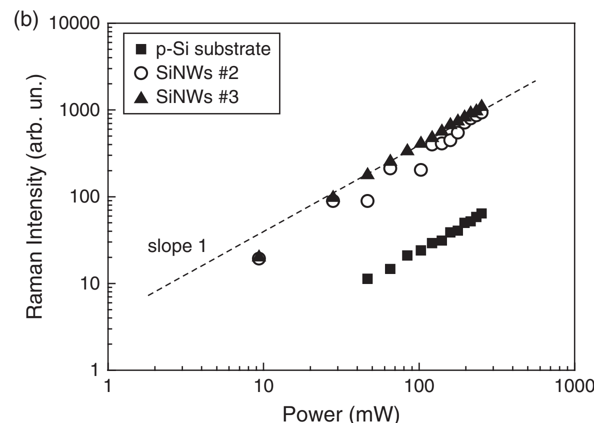

Fig. 5. Intensity of the Raman scattering at 520.5 cm^{-1} versus power of the excitation light at 1064 nm for SiNWs samples #1 (a) and #2, #3 (b) and that for the corresponding substrates. Dashed lines represent linear dependences.

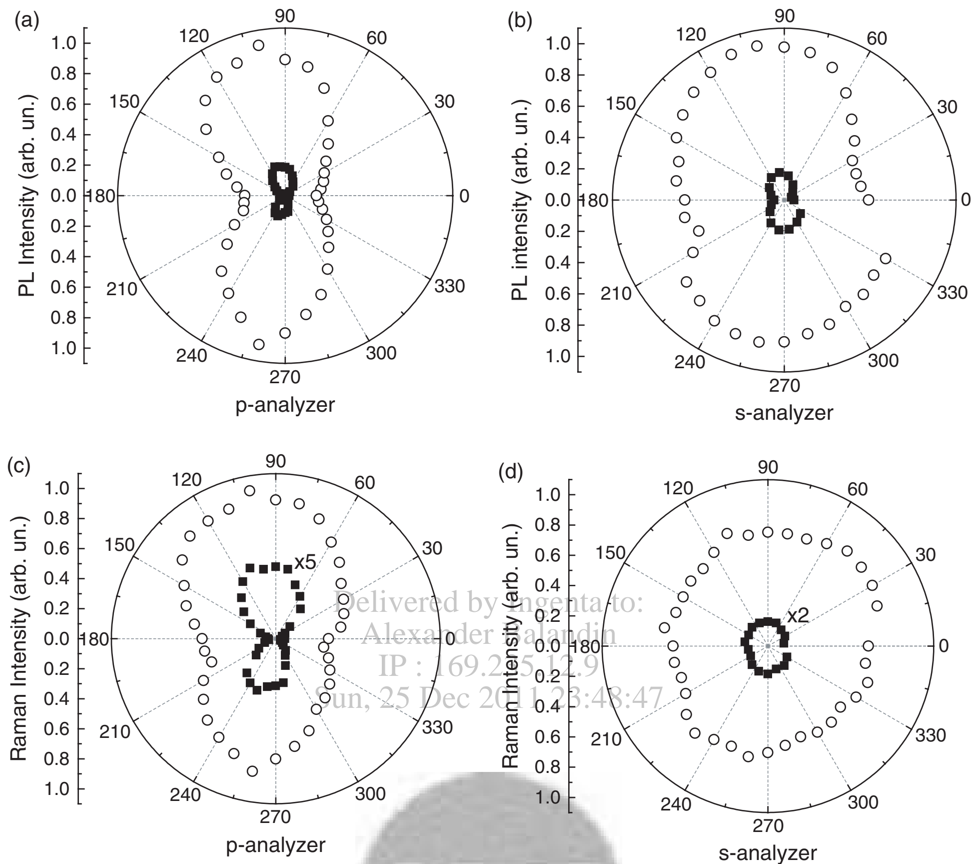

Delivered by Ingenta to:
Alexander Balandin
IP : 169.235.12.9
Sun, 25 Dec 2011 23:48:47

Fig. 6. Polarization dependences of the photoluminescence (a, b) and Raman scattering (c, d) intensities for SiNWs sample #3 (open circles) and its substrate (solid squares) measured under excitation at 1064 nm for the angle of incidence of 75 deg. The polarization angles of 0 and 90 degrees correspond to *s*- and *p*-polarization of the excitation radiation, respectively.

recombination,[18] which should stronger control the concentration of photoexcited charge carriers in the samples with lower concentration of equilibrium charge carriers.[19]

Dependences of the Raman signal after subtraction of the PL onsets on the excitation laser power are shown in Figure 5. The Raman peak intensity depends on the laser power almost linearly both for the samples and substrates of heavily and slightly doped *c*-Si. The linear dependence of the Raman scattering intensity indicates the spontaneous origin of the light as well the negligible effect of laser-induced heating in the investigated samples. The intensity of Raman scattering of the SiNW samples was by about 5 (sample #1) or above 15 (samples #2, #3) times larger than that for the corresponding substrates. This enhancement of the Raman scattering intensity demonstrates significant modifications of the interaction efficiency of the employed laser irradiation and Si nanowires in comparison with that for the bulk *c*-Si.

Discussing the results obtained under excitation at 1064 nm one should take into account the geometrical parameters and morphology of the investigated samples. The thickness of SiNW layer was about 25–40 μm (see Table I). The absorption coefficient at 1064 nm in the undoped bulk *c*-Si does not exceed 100 cm^{-1} (see Ref. [20] for example). Thus, the light absorption does not prevent whole SiNWs array from taking part in the PL and Raman signal generation. The absorption coefficient can be larger in heavily doped *c*-Si because of the absorption by defects and free charge carriers (Drude-like process).[21] One of the possible reasons of the PL and Raman enhancement in SiNWs in comparison with *c*-Si substrates is anti-reflecting action of the SiNW arrays. We can make some simple estimations of this effect based on effective-medium approach. The SiNWs form the effective layer with the effective refractive index n_{eff} less than one for *c*-Si (Bruggeman formula for the *c*-Si cylinder arrays[22] gives $n_{\mathrm{eff}} = 1.22$) and, thereby, it should reduce the reflection of the incident light from 0.32 to 0.24. However, these variations are not enough to increase the PL and Raman scattering signals by a factor of two or more. Thus, the anti-reflecting effect could not be the only and the most important reason for the rise of the PL and Raman scattering intensities.

Another important factor for the enhancement of the NIR PL and Raman scattering in SiNWs under excitation with the light at 1064 nm can be related to as called light localization phenomenon (light trapping). It seems that arrays of SiNWs result in strong scattering of the

excitation light, which is well known to accompany the light localization. This effect is especially expressed in the PL and Raman signals for sample #2 and sample #3, which are less doped than sample #1. In fact the significantly higher concentrations of impurities and free charge carriers should result in stronger absorption and then in larger optical losses in the latter sample.

Additional information concerning the light localization can be provided by polarization measurements of the Raman and PL signals as shown in Figure 6. The angle of incident light was chosen to be close to the Brewster angle (also known as the *polarization angle*) for *c*-Si, thus the obtained results should be very sensitive to the laser polarization. It was found that the polarization dependences of the *p*- and *s*-polarized Raman and PL signals differ significantly. Both for the *c*-Si substrates and SiNWs the *p*-polarized signals are three times higher than the *s*-polarized ones. The former signals in *c*-Si substrates demonstrate strong dependence on the polarization of the excitation light. The *s*-polarized radiation corresponds to a very low Raman and PL signals, whereas the *p*-polarized excitation results in the maximal signals those intensities were about 10 times larger than that for *s*-polarization. The samples of SiNWs arrays demonstrate significant enhancement of the intensities of PL and Raman scattering and depolarization of the polarization dependences. The partial polarization of the PL and Raman scattering emissions for the *p*-orientated analyzer indicates influence of the local field in arranged SiNWs. The preferable orientation of SiNWs perpendicular to the surface of *c*-Si substrate results in anisotropy of the local field (higher field in direction along the SiNW and less field in perpendicular direction), which can be revealed in the partial anisotropy of the PL and Raman signals. Note that similar effect was found in porous Si with form anisotropy of pores and Si nanocrystals.[17]

Delivered by Ingenta to: Alexander Balandin IP: 169.235.12.9 Sun, 25 Dec 2011 23:18:47

4. CONCLUSION

The multiply enhancement of the intensities of PL and Raman scattering in Si nanowires grown by wet-chemical etching in comparison with the corresponding *c*-Si substrates was found under excitation with wavelength of 1064 nm. The enhancement level is dependent on the doping level of the *c*-Si substrates. The observed effects can be explained by the partial light localization in Si nanowire arrays because of the strong scattering, which increases the interaction efficiency of the excitation light and Si nanowires. This effect can be proposed to use in different applications as random lasing with low generation thresholds, molecular sensors on specific molecules detected by the methods of Raman scattering and PL spectroscopy. In the latter case Si nanowire array can be served as a matrix for adsorbed/deposited guest molecules in order to increase their optical response.

Acknowledgments: V. A. Sivakov and S. H. Christiansen gratefully acknowledge financial support by the European FP7 Project ROD-SOL. This work was partially supported by the Russian Foundation for Basic Research (grants ## 11-02-01087, 11-02-01342, 11-02-90506).

References and Notes

1. Y. Cui, L. J. Lauhon, M. S. Gudiksen, J. Wang, and C. M. Lieber, *Appl. Phys. Lett.* 78, 2214 **(2001)**.
2. F. M. Ross, J. Tersoff, and M. C. Reuter, *Phys. Rev. Lett.* 95, 146104 **(2005)**.
3. A. I. Hochbaum, R. Fan, R. He, and P. Yang, *Nano Lett.* 5, 457 **(2005)**.
4. V. Schmidt, S. Senz, and U. Gösele, *Nano Lett.* 5, 931 **(2005)**.
5. X. Duan, Y. Huang, Y. Cui, J. Wang, and C. M. Lieber, *Nature* 409, 66 **(2001)**.
6. M. D. Kelzenberg, D. B. Turner-Evans, B. M. Kayes, M. A. Filler, M. C. Putnam, N. S. Lewis, and H. A. Atwater, *Nano Lett.* 8, 710 **(2008)**.
7. V. Sivakov, G. Andrä, A. Gawlik, A. Berger, J. Plentz, F. Falk, and S. H. Christiansen, *Nano Lett.* 9, 1549 **(2009)**.
8. R. S. Wagner and W. C. Ellis, *Appl. Phys. Lett.* 4, 89 **(1964)**.
9. A. G. Cullis, L. T. Canham, and P. D. J. Calcott, *Appl. Phys. Lett.* 82, 909 **(1997)**.
10. O. Bisi, S. Ossicini, and L. Pavesi, *Surf. Sci. Rep.* 38, 1 **(2000)**.
11. V. A. Sivakov, G. Brönstrup, B. Pecz, A. Berger, G. Z. Radnoczi, M. Krause, and S. H. Christiansen, *J. Phys. Chem. C* 114, 3798 **(2010)**.
12. V. A. Sivakov, F. Voigt, A. Berger, G. Bauer, and S. H. Christiansen, *Phys. Rev. B* 82, 125446 **(2010)**.
13. V. A. Sivakov, F. Voigt, G. Brönstrup, G. Bauer, and S. H. Christiansen, *Nanowires Nanotech.* 2, 91 **(2010)**.
14. C. Delerue, G. Allan, and M. Lannoo, *Phys. Rev. B* 48, 11024 **(1993)**.
15. G. Ledoux, O. Guillois, D. Porterat, C. Reynaud, F. Huisken, B. Kohn, and V. Paillard, *Phys. Rev. B.* 62, 15942 **(2000)**.
16. G. Ledoux, G. Gong, and F. Huisken, *Appl. Phys. Lett.* 79, 4028 **(2001)**.
17. D. Kovalev, M. B. Chorin, J. Diener, F. Koch, Al. L. Efros, M. Rosen, N. A. Gippius, and S. G. Tikhodeev, *Appl. Phys. Lett.* 67, 1585 **(1995)**.
18. M. G. Lisachenko, E. A. Konstantinova, V. Yu. Timoshenko, and P. K. Kashkarov, *Semicond.* 36, 325 **(2002)**.
19. E. H. S. Burhop, The Auger Effect and Other Radiationless Transitions, Cambridge Monographs on Physics, Cambridge **(1952)**.
20. M. J. Kerr and A. Cuevas, *J. Appl. Phys.* 91, 2473 **(2002)**.
21. S. M. Sze, Physics of Semiconductor Devices, John Wiley and Sons, N.Y. **(1981)**.
22. D. A. G. Bruggeman, *Ann. Phys. (Leipzig)* 24, 636 **(1935)**.

Received: 8 June 2011. Accepted: 15 July 2011.